

# GaN-Based Resonant-Cavity LEDs Featuring a Si-Diffusion-Defined Current Blocking Layer

Pinghui Sophia Yeh, Meng-Chun Yu, Jia-Huan Lin, Ching-Chin Huang,  
Yen-Chao Liao, Da-Wei Lin, Jia-Rong Fan, and Hao-Chung Kuo

**Abstract**—GaN-based resonant-cavity light-emitting diode (RCLED) featuring a Si-diffusion-defined confinement structure is reported for the first time. The charge-coupled device images exhibited round, bright spots of sizes corresponding to the diffusion-defined aperture sizes under continuous-wave high-current-density operation and at room temperature. The full widths at half maximum of the electroluminescence spectra were 2 and 1.5 nm for 10- and 5- $\mu\text{m}$ -diameter RCLEDs, respectively. A stable peak wavelength of 406.6 nm was maintained at various injection currents. The results suggest Si diffusion is an effective means to reduce aperture size. The design and fabrication of the devices are described.

**Index Terms**—Resonant-cavity light-emitting diode, GaN-based LED, current blocking layer, vertical cavity surface emitting laser.

## I. INTRODUCTION

CURRENT blocking layers (CBLs) that are used in GaN-based light-emitting diodes (LED) to spatially constrain current flow include silicon-oxide/silicon-nitride insulating layers, deeply etched mesas [1], ion implanted layers [2], Schottky barriers [3], and high-resistance contacts formed through techniques such as selective activation [4] and selective plasma treatment [5]. However, both ion implantation and deeply etched mesas generate lattice defects near the active region, whereas the other means cannot block current spreading in the p-GaN layer. Moreover, deposition of a silicon-oxide or a silicon-nitride layer of 200–300 nm thickness produce a non-planar surface which might affect the following processing such as dielectric distributed Bragg reflector (DBR) deposition and thus limit the feasible smallest opening size. Diffusion is a conventional processing technique that penetrates deeply into the wafer to define a 3D structure. Si diffusion in n-GaN has been used in power electronic devices [6], [7]. Moreover, Si diffusion in p-GaN was applied to convert p- into n-GaN in 2004 [8]. However, according

Manuscript received August 20, 2014; revised September 18, 2014; accepted October 3, 2014. Date of publication October 13, 2014; date of current version November 19, 2014. This work was supported by the Ministry of Science and Technology, Taiwan, under Grant NSC 101-2221-E-011-040 and Grant NSC 102-2221-E-011-086.

P. S. Yeh, M.-C. Yu, J.-H. Lin, C.-C. Huang, and Y.-C. Liao are with the Department of Electronic and Computer Engineering, Graduate Institute of Electro-Optical Engineering, National Taiwan University of Science and Technology, Taipei 10607, Taiwan (e-mail: pyeh@mail.ntust.edu.tw; m10102334@mail.ntust.edu.tw; m10002347@mail.ntust.edu.tw; m10002318@mail.ntust.edu.tw; m9802325@mail.ntust.edu.tw).

D.-W. Lin, J.-R. Fan, and H.-C. Kuo are with the Department of Photonics, Institute of Electro-Optical Engineering, National Chiao Tung University, Hsinchu 300, Taiwan (e-mail: davidlin1006@hotmail.com; vancscool-721@hotmail.com; hckuo@faculty.nctu.edu.tw).

Color versions of one or more of the figures in this letter are available online at <http://ieeexplore.ieee.org>.

Digital Object Identifier 10.1109/LPT.2014.2362297

to a thorough review of relevant research, GaN-based LEDs featuring a Si-diffusion-defined CBL has not yet been reported.

Compared to LEDs, RCLEDs have several advantages, including narrow spectral widths, stable peak wavelengths at various injection currents, superior directionality, high extraction efficiency, and high output-coupling efficiency due to relatively coherent light output [9]. GaN-based RCLEDs have several potential applications such as speckle-free illumination, display, visible light communication, and medical aesthetics. Numerous GaN-based RCLEDs have been reported. Studies emphasized cavity design and/or epitaxial DBR growth [10]–[14], demonstrated processing techniques [15]–[17], and reported a new emission wavelength of 390nm [18]. However, no previous studies have used Si-diffusion processing to confine the current. Moreover, for GaN-based RCLEDs which are usually grown on nonconductive sapphire substrate, the current flow is mostly horizontal that may cause current crowding [19] at the edge of the current injection aperture thereby exciting high-order transverse modes. For example, M. Diagne et al. [11] reported “the emission from the devices has been frequently observed to consist of a random distribution of micrometer sized “bright spots” whose origin appears to be due to locally enhanced injection current density.” In contrast, devices with vertical current flow configuration [10] using same 100-nm-thick indium-tin-oxide (ITO) current spreading layer did not have this problem. But employing vertical configuration required complex wafer transfer process to remove the sapphire substrate, and required precise wafer thickness control to attain the resonant cavity effect. In this letter, we investigated a potential solution. If the current confinement structure can be made very small, on the order of a few micrometers for single transverse mode operation; current crowding issue for devices on insulating substrates might be resolved. By using selective Si diffusion, a 5- $\mu\text{m}$ -diameter current confinement aperture was successfully fabricated while keeping a planar top surface for DBR deposition. To our knowledge, this is the smallest GaN-based RCLED demonstrated. (T. Moudakir et al. [18] reported fabrication of aperture sizes ranging from 5 to 200  $\mu\text{m}$ , but only reported results of large-aperture devices.)

## II. DEVICE STRUCTURE AND FABRICATION

A schematic diagram of the diffusion-defined RCLED is shown in Fig. 1. A two-inch GaN wafer was grown on a c-plane sapphire substrate by using metal-organic chemical vapor deposition. The epitaxial structure consisted of 25 pairs of AlN/GaN DBRs, 880-nm n-GaN, 10 pairs of InGaN/GaN

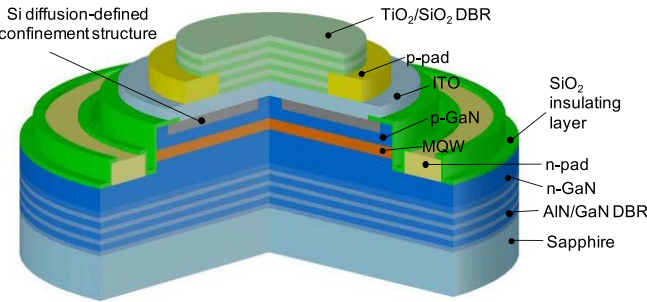


Fig. 1. 3D cross-sectional schematic diagram of the diffusion-defined RCLEDs, where DBR, ITO, MQW represent distributed Bragg reflector, indium tin oxide and multiple quantum wells, respectively.

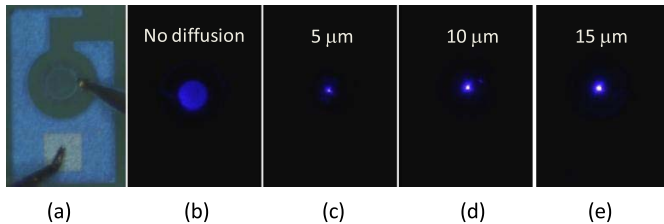


Fig. 2. CCD images in the same scale: (a) top view of the device under probe testing; (b) no-diffusion device having an ITO-defined emitting area of  $120\mu\text{m}$  in diameter; (c)  $5\mu\text{m}$ -diameter diffusion-defined device; (d)  $10\mu\text{m}$ -diameter diffusion-defined device; (e)  $15\mu\text{m}$ -diameter diffusion-defined device.

multiple quantum wells, a 25-nm-thick p-AlGaN electron blocking layer, 100-nm p-GaN, and 4-nm p-InGaN. The nominal cavity length between the AlN/GaN DBR and the wafer surface was designed to be  $7\lambda$ , where  $\lambda$  is the effective wavelength in GaN. The maximum reflectance and stopband width at 90% reflectance of the DBR were measured to be 95% and 16 nm, respectively. The device was processed as follows. A mesa structure was dry-etched to the n-GaN layer by using inductively-coupled-plasma reactive ion etching (RIE) for deploying n-contact. Then the top of the mesa was masked with a photoresist layer featuring a donut-shaped opening, and the p-GaN layer was etched approximately 20 nm by using RIE to remove the two-dimensional hole gas (2DHG) layer formed by p-InGaN/p-GaN heterostructure and to provide index guiding; subsequently, a 30-nm-thick Si thin film was deposited in sequence and then lifted off. The sample was then subjected to rapid thermal annealing at a temperature of  $800^\circ\text{C}$  in  $\text{N}_2$  ambient for 12 minutes. (Without Si diffusion, the shallow-etched region behaved as a diode with Schottky contact that can be turned on when the driving voltage was high.) The diffusion depth of Si was approximately 33 nm according to our diffusion-depth measurements using secondary ion mass spectrometer [20]. Thus, the donut region was diffused and the inner contour of the donut delineated the central aperture; the central apertures varied in size from 5 to  $15\mu\text{m}$  in diameter. One column of diodes was protected from the 2DHG-layer etching and Si diffusion to be used for comparison. Subsequently, n-pad metal ( $\text{Ti}/\text{Al}/\text{Ti}/\text{Au}$ ), a  $\text{SiO}_2$  insulating layer, and a 30-nm-thick ITO transparent conducting layer were selectively deposited in turn as shown in Fig. 1. CCD imaging was performed before p-metal deposition to record the light distribution when no metal blocking was applied. As shown in Fig. 2, the p-contact probe was placed

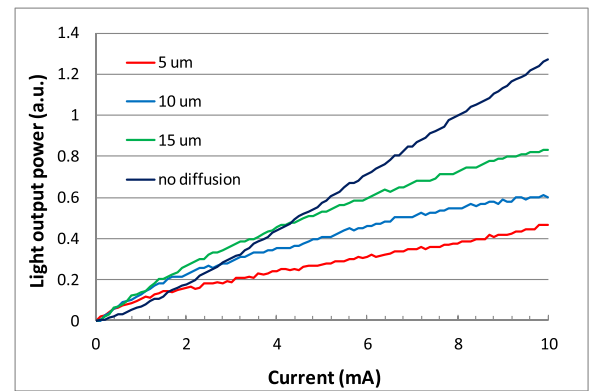


Fig. 3. L-I characteristics of the LEDs without and with diffusion-defined apertures of diameters: 5, 10 and  $15\mu\text{m}$ .

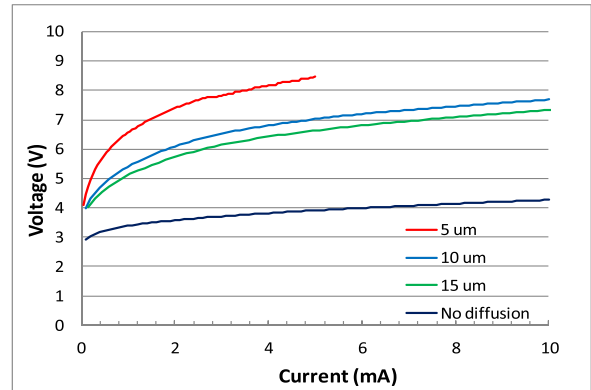


Fig. 4. V-I characteristics of the LEDs without and with diffusion-defined apertures of diameters: 5, 10 and  $15\mu\text{m}$ .

on the edge of the ITO pad at a constant current of 10 mA and at room temperature; the reference diode that was not subjected to diffusion exhibited a blurred spot with a size corresponding to the size of the ITO pad, which was  $120\mu\text{m}$  in diameter, whereas the diodes subjected to diffusion exhibited bright, round spots with sizes related to their diffusion-defined aperture sizes (the CCD was saturated in the spot region and its resolution was barely sufficient). Diffusion-confined diodes exhibited obviously higher luminance. The L-I curves are shown in Fig. 3. At low injection currents, the small-aperture devices had high current densities as well as high population inversion; thus their slope efficiencies were higher than that of the no-diffusion diode. When the injection current was continuously increased, heating and saturation problems caused gradual decrease in slope efficiency; and thus the no-diffusion diode exhibited a high slope efficiency when the injection current was greater than approximately 4 mA. (An injection current of 4 mA corresponded to current densities of 20, 5.1, 2.3 and  $0.035\text{ kA/cm}^2$  for the 5-, 10-, 15- and  $120\mu\text{m}$ -diameter diodes, respectively.) On top of the ITO pad, p-pad metal ( $\text{Ni}/\text{Au}$ ) shaped in an annular ring, with an inner diameter of  $40\mu\text{m}$  and an outer diameter of  $110\mu\text{m}$ , was deposited. The V-I characteristics were measured as shown in Fig. 4. The no-diffusion  $120\mu\text{m}$ -diameter RCLED exhibited a turn-on voltage of approximately 3.0 V and a series resistance of approximately  $71\Omega$ , indicating favorable processing quality. All Si-diffused devices exhibited

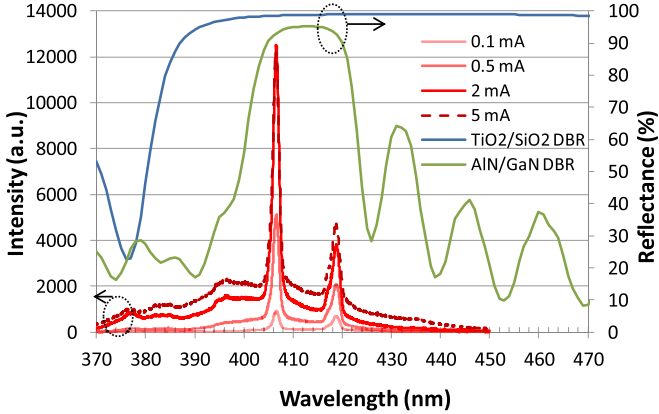


Fig. 5. Emission spectra of a 5- $\mu\text{m}$ -diameter RCLED at various currents and at room temperature. And the second y-axis vs. x-axis shows the reflectance vs. wavelength of the top and bottom DBR mirrors.

a relatively high turn-on voltage of approximately 4 V resulting from the voltage difference between the p-metal ring and the central aperture; this was because the current was forced to flow laterally through the thin ITO layer to reach the aperture region. Finally, an 8-pair  $\text{TiO}_2/\text{SiO}_2$  dielectric DBR was coated on top of the ITO layer using an e-gun evaporation system with in-situ optical monitoring to control the layer thickness. The maximum reflectance and stopband width at 90% reflectance of the DBR were 99% and 120 nm, respectively.

### III. EXPERIMENTAL RESULTS AND DISCUSSION

Emission spectra of various aperture sizes at various current injection levels were measured using a 0.1-nm-resolution optical spectrum analyzer (OSA). The analyzer's fiber was placed at a normal direction to the wafer plane. The collection area was one degree at a subtended angle or  $2.39 \times 10^{-4}$  steradian at a solid angle. As the aperture size was incrementally reduced from 15 to 10 to 5  $\mu\text{m}$ , the resonant cavity modes became more prominent; specifically, the peak/valley ratio increased and the corresponding full-width-at-half-maximum (FWHM) of the primary peak decreased from 7.0 to 2.1 to 1.9 nm, respectively, at a current of 5 mA (the FWHM of the no-diffusion RCLED was approximately 23 nm). Fig. 5 shows the representative emission spectra of a 5- $\mu\text{m}$ -diameter RCLED at various current levels. It exhibited a stable peak wavelength of  $406.6 \pm 0.05$  nm at various currents, and a large peak/valley ratio exceeding eight that indicated a strong resonance effect. Also shown on Fig. 5 are the reflectance spectra of the top and bottom DBR mirrors measured from a monitoring sample and the same epitaxial wafer, respectively. Two longitudinal modes resonated within the DBR stopband with a mode spacing of 11.1 nm, implying an effective cavity length of near 3  $\mu\text{m}$  that was attributed to the evanescent penetration of the electric field into the Bragg mirrors. At a current of 2 mA ( $10.2 \text{ kA/cm}^2$  in current density), the FWHM of the emission peak reached its minimum value of 1.5 nm; when the current was continuously increased, the secondary cavity mode at a longer wavelength

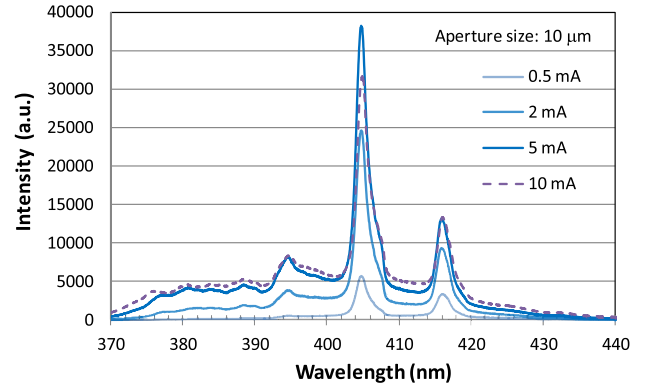


Fig. 6. Emission spectra of a 10- $\mu\text{m}$ -diameter RCLED at various currents and at room temperature.

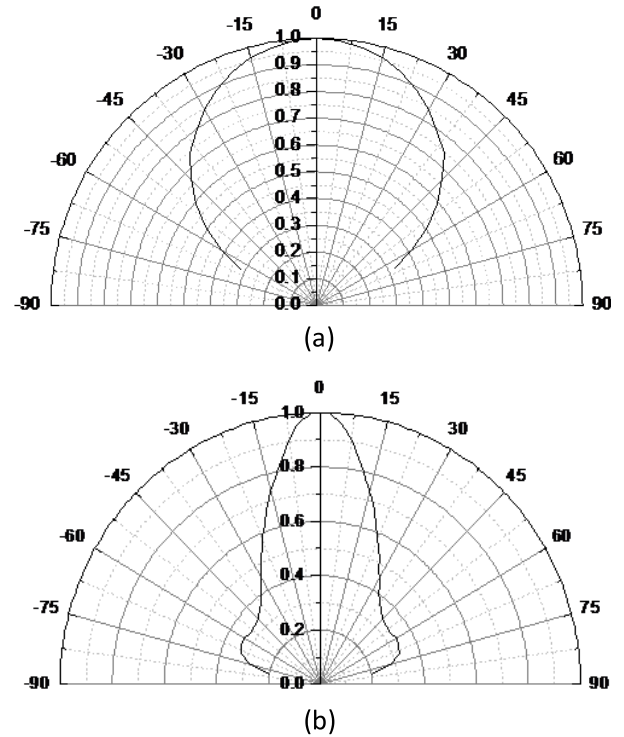


Fig. 7. Comparison of the far-field patterns of (a) 10- $\mu\text{m}$ -diameter LED and (b) 10- $\mu\text{m}$ -diameter RCLED at a current of 2 mA.

began to get more gain than the primary mode due to heating-caused red-shift of the gain curve. Fig. 6 shows the representative emission spectra of a 10- $\mu\text{m}$ -diameter RCLED at various current levels. The resonant peak wavelength remained stable at  $404.7 \pm 0.05$  nm. At a current of 2 mA ( $2.55 \text{ kA/cm}^2$  in current density), the FWHM of the primary peak reached its minimum value of 2.0 nm. When the current was continuously increased, more transverse modes appeared and broadened the FWHM. Such broadening was not seen in 5- $\mu\text{m}$ -diameter devices when driven at as high current density as 10- $\mu\text{m}$ -diameter devices. In addition, Fig. 7(a) and (b) show the far-field patterns of 10- $\mu\text{m}$ -diameter LED and RCLED, respectively, measured by an angle-resolved electroluminescence measurement system. In comparison, the

RCLED has a much smaller half-power angle of approximately 27°, because the resonant cavity effect increased the directionality of its light waves, thereby increasing the extraction efficiency. Similarly, the half-power angle of a 5- $\mu\text{m}$ -diameter RCLED measured was approximately 30°. Furthermore, the output powers of the RCLEDs were low at present, because the transmittance of the top DBR mirror was very low which can be optimized in the future.

#### IV. CONCLUSION

We fabricated and demonstrated GaN-based RCLEDs featuring a Si-diffusion-defined confinement structure. The spatial and spectral characteristics of the RCLEDs were measured. The CCD images exhibited round, bright spots of sizes corresponding to the diffusion-defined aperture sizes under CW high-current-density operation and at room temperature. The FWHM of the emission spectra were 2.0 and 1.5 nm for 10- and 5- $\mu\text{m}$ -diameter RCLEDs, respectively. The resonant peak wavelengths remained very stable (limited by 0.1-nm resolution of OSA) at various injection currents. And the far-field patterns exhibited half-power angles of 27° and 30° for 10- and 5- $\mu\text{m}$ -diameter RCLEDs, respectively, indicating superior directionality than conventional LEDs. The results suggest that Si diffusion is an effective means to reduce aperture size. The smallest GaN-based RCLED was demonstrated. It may pave the way for making single-mode GaN-based vertical cavity surface emitting lasers.

#### REFERENCES

- [1] C. Huh, J.-M. Lee, D.-J. Kim, and S.-J. Park, "Improvement in light-output efficiency of InGaN/GaN multiple-quantum well light-emitting diodes by current blocking layer," *J. Appl. Phys.*, vol. 92, no. 5, pp. 2248–2250, 2002.
- [2] M.-A. Tsai *et al.*, "Improving light output power of the GaN-based vertical-injection light-emitting diodes by Mg<sup>+</sup> implanted current blocking layer," *IEEE Photon. Technol. Lett.*, vol. 21, no. 11, pp. 688–690, Jun. 1, 2009.
- [3] T.-M. Chen *et al.*, "Current spreading and blocking designs for improving light output power from the vertical-structured GaN-based light-emitting diodes," *IEEE Photon. Technol. Lett.*, vol. 20, no. 9, pp. 703–705, May 1, 2008.
- [4] C.-M. Lee, C.-C. Chuo, Y.-C. Liu, I.-L. Chen, and J.-I. Chyi, "InGaN-GaN MQW LEDs with current blocking layer formed by selective activation," *IEEE Electron Device Lett.*, vol. 25, no. 6, pp. 384–386, Jun. 2004.
- [5] H.-Y. Lee, K.-H. Pan, C.-C. Lin, Y.-C. Chang, F.-J. Kao, and C.-T. Lee, "Current spreading of III-nitride light-emitting diodes using plasma treatment," *J. Vac. Sci. Technol. B, Microelectron. Nanometer Struct.*, vol. 25, no. 4, pp. 1280–1283, Jul. 2007.
- [6] S. Jang *et al.*, "Si-diffused GaN for enhancement-mode GaN MOSFET on Si applications," *J. Electron. Mater.*, vol. 35, no. 4, pp. 685–690, 2006.
- [7] Y.-W. Lian, Y.-S. Lin, J.-M. Yang, C.-H. Cheng, and S. S. H. Hsu, "AlGaN/GaN Schottky barrier diodes on silicon substrates with selective Si diffusion for low onset voltage and high reverse blocking," *IEEE Electron Device Lett.*, vol. 34, no. 8, pp. 981–983, Aug. 2013.
- [8] C. J. Pan, G. C. Chi, B. J. Pong, J. K. Sheu, and J. Y. Chen, "Si diffusion in p-GaN," *J. Vac. Sci. Technol. B, Microelectron. Nanometer Struct.*, vol. 22, no. 4, pp. 1727–1730, Jul. 2004.
- [9] E. F. Schubert, Y.-H. Wang, A. Y. Cho, L.-W. Tu, and G. J. Zydzik, "Resonant cavity light-emitting diode," *Appl. Phys. Lett.*, vol. 60, no. 8, pp. 921–923, 1992.
- [10] Y.-K. Song, M. Diagne, H. Zhou, A. V. Nurmikko, R. P. Schneider, Jr., and T. Takeuchi, "Resonant-cavity InGaN quantum-well blue light-emitting diodes," *Appl. Phys. Lett.*, vol. 77, no. 12, pp. 1744–1746, 2000.
- [11] M. Diagne *et al.*, "Vertical cavity violet light emitting diode incorporating an aluminum gallium nitride distributed Bragg mirror and a tunnel junction," *Appl. Phys. Lett.*, vol. 79, no. 22, pp. 3720–3722, 2001.
- [12] C. F. Lin, H. H. Yao, J. W. Lu, Y. L. Hsieh, H. C. Kuo, and S. C. Wang, "Characteristics of stable emission GaN-based resonant-cavity light-emitting diodes," *J. Cryst. Growth*, vol. 261, nos. 1–3, pp. 359–363, Jan. 2004.
- [13] J. Dorsaz, J.-F. Carlin, C. M. Zellweger, S. Gradecak, and M. Illegems, "InGaN/GaN resonant-cavity LED including an AlInN/GaN Bragg mirror," *Phys. Status Solidi A*, vol. 201, pp. 2675–2678, 2004.
- [14] T.-C. Lu *et al.*, "GaN-based high-Q vertical-cavity light-emitting diodes," *IEEE Electron Device Lett.*, vol. 28, no. 10, pp. 884–886, Oct. 2007.
- [15] R.-H. Horng, W.-K. Wang, S.-Y. Huang, and D.-S. Wuu, "Effect of resonant cavity in wafer-bonded green InGaN LED with dielectric and silver mirrors," *IEEE Photon. Technol. Lett.*, vol. 18, no. 3, pp. 457–459, Feb. 1, 2006.
- [16] S.-Y. Huang, R.-H. Horng, P.-H. Tseng, J.-H. Tu, L.-W. Tu, and D.-S. Wuu, "Study on hydrogen ion-implanted characteristic of thin-film green resonant-cavity light-emitting diodes," *IEEE Photon. Technol. Lett.*, vol. 22, no. 6, pp. 404–406, Mar. 15, 2010.
- [17] X.-L. Hu *et al.*, "Fabrication and characterization of high-quality factor GaN-based resonant-cavity blue light-emitting diodes," *IEEE Photon. Technol. Lett.*, vol. 24, no. 17, pp. 1472–1474, Sep. 1, 2012.
- [18] T. Moudakir *et al.*, "Design, fabrication, and characterization of near-milliwatt-power RCLEDs emitting at 390 nm," *IEEE Photon. J.*, vol. 5, no. 6, Dec. 2013, Art. ID 8400709.
- [19] E. F. Schubert, *Light-Emitting Diodes*. Cambridge, U.K.: Cambridge Univ. Press, 2006, ch. 8.
- [20] J.-H. Lin, "Research on GaN-based vertical cavity surface emitting diodes with diffusion-defined confinement structure," M.S. thesis, Dept. Electron. Comput. Eng., Nat. Taiwan Univ. Sci. Technol., Taipei, Taiwan, 2013.